

# COSMOLOGICAL CONSTRAINTS ON HOLOGRAPHIC DARK ENERGY MODELS UNDER THE ENERGY CONDITIONS

MING-JIAN ZHANG<sup>1</sup>, ZHONG-XU ZHAI<sup>2</sup>, CONG MA<sup>1</sup>, TONG-JIE ZHANG<sup>1,3</sup>

*Draft version March 5, 2013*

## Abstract

We study the holographic and agegraphic dark energy models with the observational Hubble parameter data (OHD), the Union2 data set of type Ia supernovae (SNIa), and the energy conditions. Scenarios of dark energy are distinguished by the cut-off of cosmic age, conformal time, and event horizon. The joint constraint from observational data gives  $\Omega_{m0} = 0.22 \pm 0.03$ , and  $c > 5.92$  for age cut-off,  $\Omega_{m0} = 0.2 \pm 0.03$ , and  $c > 6.43$  for conformal time cut-off, and  $\Omega_{m0} = 0.22^{+0.04}_{-0.05}$ , and  $c = 0.84^{+0.14}_{-0.12}$  for event horizon cut-off. Our results show that the two former models finally reduce to  $\Lambda$ CDM model, but the latter is different from  $\Lambda$ CDM model. Comparing with the energy conditions, we find that SEC is fulfilled at redshift  $z \gtrsim 0.3$  with  $1\sigma$  confidence level, and  $z \gtrsim 0.5$  with  $3\sigma$  confidence level, which is well consistent with the result reported by Wu et al. (2012). Notably the null energy condition is showed to closely track the data constraints, thereby distinguishes itself from other energy conditions.

*Subject headings:* cosmology: theory — dark energy — cosmology: observations

## 1. INTRODUCTION

An accelerated expansion of the universe is suggested by independent cosmological probes such as the supernova (SN) Ia observations (Riess et al. 1998), large scale structure (Tegmark et al. 2004), and cosmic microwave background anisotropies (CMB) (Spergel et al. 2003). Dark energy models are generally perceived as theoretical explanations of this acceleration. Observations such as the 2dFGRS, the SDSS, CMB measurements and other cosmological data show that our universe consists of about 5% normal matter, 25% dark matter, and 70% dark energy. When it comes to the 70% dark energy, theories are always active in the front. Many candidates are proposed for an interpretation of the dark energy, including the cosmological constant, quintessence (Peebles & Ratra 1988), K-essence (Armendariz-Picon et al. 2000), tachyon (Padmanabhan 2002), phantom (Caldwell et al. 2003), ghost condensate (Piazza 2004) and quintom (Feng et al. 2005). Despite the effort on a viable theoretical formulation of dark energy, its nature remains open to interpretations.

The confrontation of theories and data, however, is not all one may perform in the face of the proliferation of dark energy proposals. One of the many interesting approaches makes use of the so-called *energy conditions*. These conditions were introduced by Hawking et al. (1975) as coordinate-invariant inequality constraints on the energy-momentum tensor that appears in the Einstein field equation. Due to their simplicity and model independence, the energy conditions are frequently discussed in the general context of gravitation (Wald 1984). Of the many proposed energy conditions, the ones we employ in this paper are the null, weak, strong, and dominant energy conditions (abbreviated respectively as NEC, WEC, SEC, and DEC). The energy conditions in the setting of a homogeneous and isotropic Friedmann-Robertson-Walker (FRW) universe

summarized by Carroll (2004, Chapter 4) can be expressed in terms of the energy density  $\rho$  and the pressure  $p$  as following:

$$\begin{aligned} \text{NEC} : \quad & \rho + p \geq 0, \\ \text{WEC} : \quad & \rho \geq 0 \quad \text{and} \quad \rho + p \geq 0, \\ \text{SEC} : \quad & \rho + 3p \geq 0 \quad \text{and} \quad \rho + p \geq 0, \\ \text{DEC} : \quad & \rho \geq 0 \quad \text{and} \quad -\rho \leq p \leq \rho. \end{aligned} \tag{1}$$

The energy conditions have been useful in discussing the general property of fluid models (Wu et al. 2012, and references therein). The energy conditions were applied to cosmology by Visser (1997a,b, 2000). It has been shown that constraints on a variety of cosmological variables or parameters can be predicted from the energy conditions, such as the Hubble parameter, luminosity and angular diameter distances, lookback time (Visser 1997b), total density parameter  $\Omega(z)$ , energy density  $\rho(z)$ , and pressure  $p(z)$  (Cattoën & Visser 2008). In a word, the energy conditions have been an useful tool for our understanding of the Universe's evolution.

Unlike first-principle laws of physics, the energy conditions are not expected to hold *a priori*, nor are they found to do so from data. It has been shown that the WEC and DEC are fulfilled for  $z \leq 1$  and  $z \lesssim 0.8$  by supernova data with  $3\sigma$  confidence levels, respectively (Lima et al. 2008). Nevertheless, SEC violation is a typical trait of a positive cosmological constant  $\Lambda$  (Li et al. 2011) and other dark energy models (Schuecker et al. 2003). It is also said that the WEC violate the quantum field theory due to arbitrarily negative renormalized energy density may occur at some points of spacetime (Epstein et al. 1965). If extended regions of large negative energy density emerge in the nature, exotic and possibly undesirable phenomena may be allowed, ranging from violations of the second law of thermodynamics and cosmic censorship to the creation of time machines and warp drives (Fewster et al. 1998).

Recently, Wu et al. (2012) studied the likelihood of energy condition violations in the history of the universe. They found that the data suggest a fulfillment of null and dominant en-

tjzhang@bnu.edu.cn

<sup>1</sup> Department of Astronomy, Beijing Normal University, Beijing 100875, China

<sup>2</sup> Department of Physics, Institute of Theoretical Physics, Beijing Normal University, Beijing, 100875, China

<sup>3</sup> Center for High Energy Physics, Peking University, Beijing 100871, China

ergy conditions, but a violation of strong energy condition, especially for low redshift ( $z \leq 0.3$ ). They also noted the difficulty of assessing the possibility of SEC violation at the high redshift. Moreover, their result for SEC hints at a recent transition from deceleration to acceleration with the transition redshift  $z \approx 0.5$  under the ignorance of bias at the high redshift. Therefore, the SEC fulfillment appears disfavored as a test for cosmological models. On the contrary, a dark energy model is expected to reproduce its violation for recent eras of cosmic evolution.

We shall in this paper analyse a set of dark energy models from the holographic family in the context of energy conditions. The models are based on the holographic principle (Li 2004) with inspiration drawn from the Bekenstein entropy bound. In an effective quantum field theory, the total entropy in a box of size  $L$  with UV cut-off  $\Lambda$  relating to the quantum zero-point energy (Susskind 1995; 't Hooft 2001) should satisfy the relation

$$L^3 \Lambda^3 \leq S_{BH} \equiv \pi M_p^2 L^2, \quad (2)$$

where  $S_{BH}$  is the entropy of a black hole within the same size as  $L$ , and  $M_p \equiv 1/\sqrt{8\pi G}$  is the reduced Planck mass. Cohen et al. (1999) suggested that a short distance cut-off in quantum field theory is related to a long distance cut-off, due to the limit set by formation of a black hole. If  $\rho_\Lambda$  is the quantum zero-point energy density caused by a short distance cut-off, the total energy in a region of size  $L$  should not exceed the mass of a black hole of the same size, namely,  $L^3 \rho_\Lambda \leq LM_p^2$ . The largest  $L$  allowed is the one saturating this inequality. Therefore, the zero-point energy density should satisfy (Li 2004)

$$\rho_\Lambda = 3c^2 M_p^2 L^{-2}. \quad (3)$$

Here,  $c$  is a dimensionless constant indicating the abundance of matter or dark energy component. It should not be confused with the speed of light. The choice of the cut-off  $L$  serves to distinguish different models within the holographic family, and several cosmological scales have been proposed as the cut-off. Models corresponding to spatial scales, e. g. the Hubble horizon, the particle horizon or the event horizon, are customarily called holographic dark energy models; other models corresponding to temporal scales, e. g. the age of the universe or the conformal time, are dubbed agegraphic dark models. The agegraphic dark energy model is also pointed out to be classically unstable (Kim et al. 2008). In addition, the determination of constant  $c$  is still a difficult problem in some of these models.

This paper is organized as follows: In Sec. 2 the basic expansion rate for general holographic and agegraphic dark energy models (collectively abbreviated as HDE) is derived and calculated for different choices of the IR cut-off. Proceeding to Sec. 3 we subject the models to our data constraints and energy condition analyses. Our main results and discussions are presented in Sec. 4.

## 2. HOLOGRAPHIC AND AGEGRAPHIC DARK ENERGY MODELS

In this section we consider the HDE models without interaction (Wu et al. 2008) between the dark energy and matter (including both baryon matter and cold dark matter). The Friedmann equation for a spatially flat FRW model ignoring the radiation reads (Li 2004; Zhang & Wu 2007)

$$\rho_m + \rho_\Lambda = 3M_p^2 H^2. \quad (4)$$

By introducing  $\Omega_m = \rho_m/(3M_p^2 H^2)$  and  $\Omega_\Lambda = \rho_\Lambda/(3M_p^2 H^2)$ , the Friedmann equation can also be cast as  $\Omega_m + \Omega_\Lambda = 1$ . With the dark energy pressure  $p = \omega\rho$  and cold dark matter pressure  $p = 0$ , the total pressure  $p$  is given by

$$p = 3M_p^2 \omega c^2 L^{-2}, \quad (5)$$

where  $\omega$  is called the equations of state (EoS) parameter. Following previous works (Li 2004; Setare 2006; Zhai et al. 2011; Chen et al. 2011), the continuity equations for dark energy and matter respectively are

$$\dot{\rho}_m + 3H(1 + \omega_m)\rho_m = 0, \quad \dot{\rho}_\Lambda + 3H(1 + \omega_\Lambda)\rho_\Lambda = 0, \quad (6)$$

where a dot above denotes the derivative with respect to the cosmic time  $t$ . Connecting Eqs. (4) and (6) we can obtain

$$2M_p^2 \dot{H} + 3M_p^2 H^2 + \omega_m \rho_m + \omega_\Lambda \rho_\Lambda = 0. \quad (7)$$

By virtue of  $\omega_m = 0$ , the EoS of HDE, with the help of the second equation of Eq. (6), can be expressed as

$$\begin{aligned} \omega_\Lambda &= -1 - \frac{1}{3H} \frac{\dot{\rho}_\Lambda}{\rho_\Lambda} = -1 - \frac{1}{3H\Omega_\Lambda} \left( \frac{2\Omega_\Lambda}{H} \frac{dH}{dt} + \frac{d\Omega_\Lambda}{dt} \right) \\ &= -1 - \frac{2}{3} \left( \frac{d \ln H}{d \ln a} + \frac{1}{2} \frac{d \ln \Omega_\Lambda}{d \ln a} \right). \end{aligned} \quad (8)$$

Applying the EoS of HDE, Eq. (7) reduces to

$$\frac{d \ln H}{d \ln a} - \frac{1}{2} \frac{\Omega_\Lambda}{(1 - \Omega_\Lambda)} \frac{d \ln \Omega_\Lambda}{d \ln a} + \frac{3}{2} = 0. \quad (9)$$

Meanwhile, we get the Hubble parameter  $H(z) = H_0 E(z)$  with Eq. (8) and Friedmann equation Eq. (4), where the expansion rate  $E(z)$  is given by (Zhai et al. 2011)

$$E^2(z) = \Omega_{m0}(1+z)^3 + \Omega_{\Lambda 0} \exp \left[ 3 \int_0^z \frac{1 + \omega_\Lambda(z')}{1+z'} dz' \right]. \quad (10)$$

Here the subscript “0” denotes the present value of a quantity.

To further quantify a model, a choice of the IR cut-off is needed. Scenarios summarized by Chen et al. (2011) contains the Hubble horizon, the particle horizon, the event horizon, the age of the universe and the conformal time (Xu et al. 2010; Zhai et al. 2011). However, an accelerating expansion of the universe cannot be achieved when the Hubble horizon or the particle horizon is chosen as the IR cut-off. In this paper, we mainly aim at the last three scenarios. Recently, Zhai et al. (2011) investigated four of them and found that the event horizon is more preferable than Hubble horizon scenario. However, both two temporal scenarios better recovers the  $\Lambda$ CDM model than the spatial scenarios. In our following calculations we shall choose such dimensions and units that the speed of light  $c_L = 1$ . Our final results will be presented in dimensionless quantities.

### 2.1. Cosmic age cut-off

The first scenario, the cosmic age cut-off, is defined as

$$t_\Lambda = \int_0^t dt' = \int_0^a \frac{da'}{Ha'}. \quad (11)$$

In this case, the age of universe is considered as a time scale. The corresponding spatial scale is obtained after multiplication by the speed of light, which we have chosen to be  $c_L = 1$ . According to Eq. (3) the resulting dark energy density is

$$\rho_\Lambda = 3c^2 M_p^2 t_\Lambda^{-2}. \quad (12)$$

With the dark energy density parameter  $\Omega_\Lambda = \rho_\Lambda/(3M_p^2 H^2)$  and the definition Eq. (11), one finds

$$\int_0^a \frac{d \ln a'}{H} = \frac{c}{H} \sqrt{\frac{1}{\Omega_\Lambda}}. \quad (13)$$

Taking the derivative with respect to  $\ln a$ , a differential equation is derived

$$\frac{d \ln H}{d \ln a} + \frac{1}{2} \frac{d \ln \Omega_\Lambda}{d \ln a} + \frac{\sqrt{\Omega_\Lambda}}{c} = 0. \quad (14)$$

Then, from Eqs. (9) and (14), the evolution of  $\Omega_\Lambda$  can be found to satisfy

$$\frac{d \Omega_\Lambda}{dz} = -2\Omega_\Lambda(1 - \Omega_\Lambda) \left( \frac{3}{2} - \frac{\sqrt{\Omega_\Lambda}}{c} \right) (1+z)^{-1}. \quad (15)$$

Meanwhile, the EoS for HDE can be obtained from Eqs. (8) and (14)

$$\omega_\Lambda = \frac{2}{3c} \sqrt{\Omega_\Lambda} - 1. \quad (16)$$

Accelerated expansion requires  $c > \sqrt{\Omega_\Lambda}$  in order to satisfy  $\omega < -1/3$ . When the constant  $c$  approaches infinity, the  $\Lambda$ CDM model is recovered. The expansion rate under this scenario can eventually be determined by Eqs. (10) and (16).

### 2.2. Conformal time cut-off

The second scenario we shall consider is the conformal time as the IR cut-off. It is in the form

$$\eta_\Lambda = \int_0^t \frac{dt'}{a} = \int_0^a \frac{da'}{Ha'^2}, \quad (17)$$

which is the total comoving distance that light could travel (Myung & Seo 2009). In this case, the conformal time is considered as a temporal scale, and we can again convert it to a spatial scale to be used as the IR cut-off  $L$ . Analogous to Section 2.1 we obtain a differential expression of  $\Omega_\Lambda$  with respect to  $\ln a$ :

$$\frac{d \ln H}{d \ln a} + \frac{1}{2} \frac{d \ln \Omega_\Lambda}{d \ln a} + \frac{\sqrt{\Omega_\Lambda}}{ac} = 0. \quad (18)$$

We can go further with the aid of Eq. (9):

$$\frac{d \Omega_\Lambda}{dz} = -2\Omega_\Lambda(1 - \Omega_\Lambda) \left[ \frac{3}{2}(1+z)^{-1} - \frac{\sqrt{\Omega_\Lambda}}{c} \right]. \quad (19)$$

The EoS for HDE can be obtained from Eqs. (8) and (18)

$$\omega_\Lambda = \frac{2}{3} \frac{\sqrt{\Omega_\Lambda}}{c} (1+z) - 1, \quad (20)$$

which corresponds an acceleration when  $c > \sqrt{\Omega_\Lambda}(1+z)$ . With  $c \rightarrow \infty$  it will also recover the  $\Lambda$ CDM model. The corresponding expansion rate Eq. (10) of this scenario can also be solved.

### 2.3. Event horizon cut-off

For our last model, we consider the event horizon (Bhattacharya & Debnath 2011) given by

$$R_E = a \int_t^\infty \frac{dt'}{a(t')} = a \int_a^\infty \frac{da'}{Ha'^2}, \quad (21)$$

which is the boundary of the volume a fixed observer may eventually observe. We now identify this scale as the cut-off length  $L$  as it appears in Eq. (3). With the introduction of dark energy density parameter  $\Omega_\Lambda$ , and performing the same analysis, we obtain the relation from Eq. (21)

$$\int_0^a \frac{d \ln a'}{Ha'} = \frac{c}{Ha} \sqrt{\frac{1}{\Omega_\Lambda}}. \quad (22)$$

Taking the derivative with respect to  $\ln a$  of Eq. (22), we get a differential equation

$$\frac{d \ln H}{d \ln a} + \frac{1}{2} \frac{d \ln \Omega_\Lambda}{d \ln a} = \frac{\sqrt{\Omega_\Lambda}}{c} - 1. \quad (23)$$

In this manner we further obtain the evolution of  $\Omega_\Lambda$  from the above Eqs. (9) and (23)

$$\frac{d \Omega_\Lambda}{dz} = -2\Omega_\Lambda(1 - \Omega_\Lambda) \left( \frac{1}{2} + \frac{\sqrt{\Omega_\Lambda}}{c} \right) (1+z)^{-1}. \quad (24)$$

Same as the other scenarios but for Eqs. (8) and (23), the EoS for HDE is found to be

$$\omega_\Lambda = -\frac{1}{3} \left( \frac{2}{c} \sqrt{\Omega_\Lambda} + 1 \right). \quad (25)$$

Obviously, the acceleration condition  $\omega < -1/3$  is satisfied as long as  $c > 0$ . With  $c \rightarrow \infty$ , we have  $\omega \rightarrow -1/3$ . This is distinguished from the previous two scenarios. As with the other models, the Hubble expansion rate  $E(z)$  shall follow easily.

## 3. OBSERVATIONAL CONSTRAINTS AND THE ENERGY CONDITIONS

Holographic and agegraphic dark energy models have been examined using various astronomical observations, such as SNIa (Huang & Gong 2004) and CMB (Enqvist et al. 2005), among others. Indeed, constraint on HDE from OHD is also performed (Yi & Zhang 2007; Zhai et al. 2011). Using the OHD and  $\chi^2$  statistics, the authors gave the best-fit values of parameters  $\Omega_{m0}$  and  $c$ , suggesting that  $c < 1$  is favored. Various estimations of the  $c$  parameter has been made (Huang & Gong 2004; Kao et al. 2005; Zhang & Wu 2007), however there appears to be little consensus about its precise range. The constant  $c$  is a key parameter in the HDE model which determines the evolutionary behavior of the spacetime and the ultimate fate of the Universe. In this paper, we therefore try to use the current OHD and SNIa with the energy conditions for a further study. These two datasets are sensitive to the cosmic evolution in the dark energy-dominated era and turn out to form good complementary constraints.

### 3.1. Hubble parameter

Observational Hubble parameter data (OHD) can be measured through the aging of passively evolving galaxies (Jimenez & Loeb 2002; Simon et al. 2005; Stern et al. 2010; Moresco et al. 2012) and the baryon acoustic oscillation (BAO) effect (Gaztanaga et al. 2009). Recently, four OHD points have also been obtained by adopting the differential age method from the 7th data release (DR7) of SDSS (Zhang et al. 2012). OHD have presented their value in the standard cosmological model (Lin et al. 2009; Stern et al. 2010), various other FRW models (Samushia & Ratra 2006; Zhang et al. 2010; Zhai et al. 2011), and even the Lemaître-Tolman-Bondi (LTB) void models (Wang & Zhang 2012). The potential of future OHD observations in constraining FRW models is explored via simulation in (Ma & Zhang 2011).

By the  $\chi^2$  statistics, one can get the best-fitting values of the parameters and its corresponding confident regions

$$\chi^2(H_0, z, p) = \sum_i \frac{[H_0 E(z_i) - H^{obs}(z_i)]^2}{\sigma_i^2}, \quad (26)$$

where  $p$  stands for the parameter vector of each dark energy models and  $H_0 = 74.3 \pm 2.1 \text{ km s}^{-1} \text{ Mpc}^{-1}$  is the prior which is

a 2.8% precision measurement suggested by Freedman et al. (2012).

### 3.2. Luminosity distance

We also apply a rich and widely used SIna sample, the Union2 dataset (Amanullah et al. 2010). The data are presented as tabulated distance moduli with errors. By definition, the luminosity distance modulus is the difference between the apparent magnitude  $m$  and the absolute magnitude  $M$  defined by

$$\mu^{th}(z) = m^{th}(z) - M = 5 \log D_L(z) + \mu_0, \quad (27)$$

where  $\mu_0 = 42.38 - 5 \log h$ , and  $h$  is the Hubble constant  $H_0$  in units of  $100 \text{ km s}^{-1} \text{ Mpc}^{-1}$ . The luminosity distance function  $D_L(z)$  in a flat space can be expressed as

$$D_L(z) = (1+z) \int_0^z \frac{dz'}{E(z'; p)}, \quad (28)$$

where the dimensionless Hubble expansion rate  $E(z'; p)$  is connected through Eq. (10). While the observational distance modulus is also given by

$$\mu^{obs}(z) \equiv m^{obs}(z) - M. \quad (29)$$

The parameters in theoretical models are determined by minimizing the expression

$$\chi^2(H_0, z, p) = \sum_i \frac{[\mu^{obs}(z) - \mu^{th}(z)]^2}{\sigma_i^2(z)}, \quad (30)$$

where  $\sigma_i$  is the uncertainty of distance modulus given by the data. The parameter  $\mu_0$  is a nuisance parameter but independent of the data points. Generally, one can perform a uniform marginalization over  $\mu_0$ . However, we can carry out an alternative way (Di Pietro & Claeskens 2003; Nesseris & Perivolaropoulos 2005; Perivolaropoulos 2005). The  $\chi^2$  of Eq. (30) with respect to  $\mu_0$  can be written as

$$\tilde{\chi}^2(z, p) = A - \frac{B^2}{C}, \quad (31)$$

where

$$\begin{aligned} A(p) &= \sum_i \frac{[\mu^{obs}(z) - \mu^{th}(z; \mu_0 = 0, p)]^2}{\sigma_i^2(z)}, \\ B(p) &= \sum_i \frac{\mu^{obs}(z) - \mu^{th}(z; \mu_0 = 0, p)}{\sigma_i^2(z)}, \\ C &= \sum_i \frac{1}{\sigma_i^2(z)}. \end{aligned} \quad (32)$$

By the equivalence between Eqs. (30) and (31), we can instead minimize  $\tilde{\chi}^2$  which is not explicitly dependent on  $\mu_0$ .

### 3.3. Energy conditions

By virtue of the Eqs. (3), (4) and (5), the energy conditions can be expressed in the below forms. The NEC suggests

$$1 + \omega\Omega_\Lambda \geq 0, \quad (33)$$

the WEC

$$3M_p^2 H^2 \geq 0 \quad \text{and} \quad 1 + \omega\Omega_\Lambda \geq 0, \quad (34)$$

the SEC:

$$1 + 3\omega\Omega_\Lambda \geq 0 \quad \text{and} \quad 1 + \omega\Omega_\Lambda \geq 0, \quad (35)$$

the DEC:

$$3M_p^2 H^2 \geq 0, \quad 1 + \omega\Omega_\Lambda \geq 0, \quad \text{and} \quad 1 - \omega\Omega_\Lambda \geq 0. \quad (36)$$

Because of the non-negativity of  $3M_p^2 H^2$ , WEC eventually reduces to NEC.

Assuming the energy conditions, some bounds can be placed on parameters  $\omega$  and  $\Omega_\Lambda$ . Furthermore, the EoS parameter  $\omega$  can be constructed from parameters  $\Omega_\Lambda$  (or  $\Omega_m$ ) and  $c$ , which will be shown in next section. Thus, the energy conditions actually provide a series of constraints on parameters  $\Omega_m$  and  $c$ . Note that the dark energy component  $\Omega_\Lambda$  varies with redshift  $z$ , and its evolution has been shown in the above section. This means that we cannot expect the energy conditions to be constantly fulfilled or violated.

### 3.4. Joint data constraints and energy condition bounds

Having carried out the  $\chi^2$  analysis with our three models, we are able to report the resulting constraint on the parameters, as shown by Figure 1. As can be seen from that figure, the OHD and SNIa sets display fairly good complementarity, despite some trouble with bounding the  $c$  parameter. Together they are able to reduce the parameter degeneracy and give us satisfactory bounds on  $\Omega_{m0}$  for all the three models. Even if they cannot always bound the parameter  $c$ , when used together the data improves our lower estimate of its possible range by a significant margin.

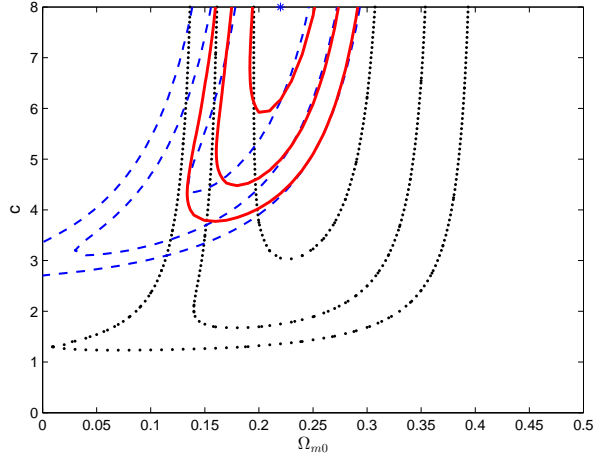
For the *cosmic age cut-off* model, we find  $\Omega_{m0} = 0.22 \pm 0.03$  and  $c > 5.92$  at 68.3% confidence level with  $\chi_{\min}^2 = 567.7$ . For this model the constant  $c$  cannot be bound from above by our data. The energy conditions bounds at redshift  $0 \leq z \leq 0.5$  are shown in Figure 2. As for the energy conditions, we find that both NEC and DEC are trivially satisfied by the constrained regions for the entire redshift range. However, the data are in tension against SEC fulfillment at redshift  $z = 0$ . In addition, we plot the evolution of the SEC bound at different redshift. We find that SEC is fulfilled at redshift  $z \gtrsim 0.3$  with  $1\sigma$  confidence level, and  $z \gtrsim 0.5$  with  $3\sigma$  confidence level, which is well consistent with the result reported by Wu et al. (2012).

For the *conformal time cut-off* model, constraints from data and the energy conditions are shown in Figure 3. The joint constraint for OHD and SN gives  $\Omega_{m0} = 0.2 \pm 0.03$  and  $c > 6.43$  at 68.3% confidence level with  $\chi_{\min}^2 = 568.4$ . NEC and DEC are almost kept stably consistently for the redshift range. This is same as the situation in age of universe cut-off. Moreover, an analogous result for SEC is obtained. That is, SEC is valid when redshift  $z \gtrsim 0.3$  for  $1\sigma$  confidence level.

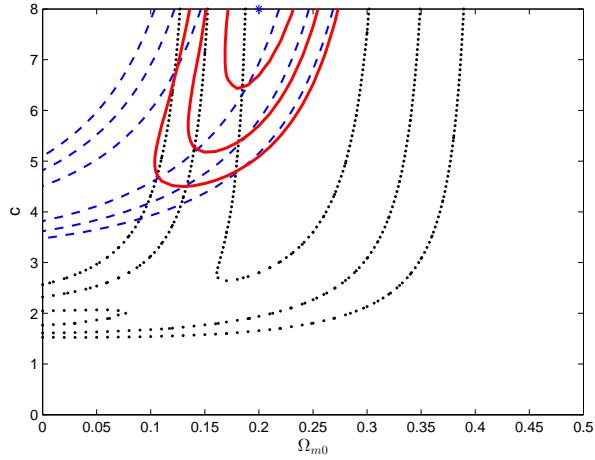
Finally we perform the  $\chi^2$  analysis on the *event horizon cut-off* model and obtain the best-fit result  $\Omega_{m0} = 0.22^{+0.04}_{-0.05}$  and  $c = 0.84^{+0.14}_{-0.12}$  at 68.3% confidence level, with  $\chi_{\min}^2 = 566.3$ . The constraint is consistent with  $c < 1$  at  $1\sigma$  confidence level. Comparison with energy condition bounds is shown in Figure 4. We note that NEC can give a much more meaningful bound for this scenario, especially at  $z = 0$ . For SEC, a familiar result is obtained, i. e. fulfill data at redshift  $z \gtrsim 0.3$  with  $1\sigma$  confidence level, and  $z \gtrsim 0.5$  with  $3\sigma$  confidence level.

## 4. CONCLUSION AND DISCUSSIONS

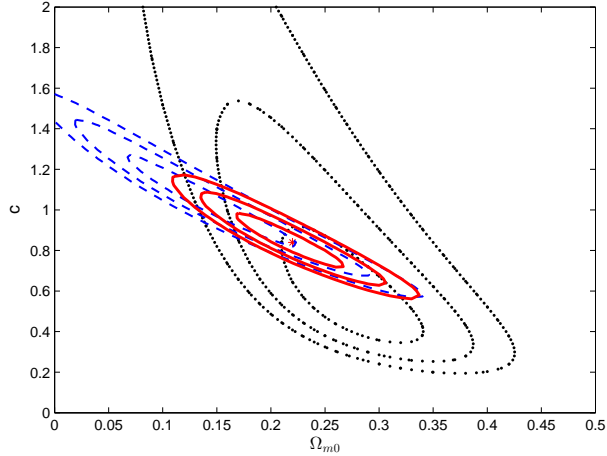
We perform  $\chi^2$  statistics using OHD and SN Union2 data set. The best-fit value of matter density for the three scenarios almost steadily located at  $\Omega_{m0} = 0.22$  with  $1\sigma$  confidence level. The main results are shown in Figure 1. It turns out that  $c$  cannot be constrained with a closed region for the age and



(a) Cosmic age



(b) Conformal time



(c) Event horizon

**Figure 1.** Constraints on parameters  $(\Omega_{m0}, c)$  from OHD and SN for the three models. The dashed and dotted contours are obtained from SN and OHD respectively. The solid contours are joint constraints for OHD and SN. The contour levels correspond to 68.3%, 95.4% and 99.7% confidence regions. In the calculation of constraint from OHD, the latest measurement  $H_0 = 74.3 \pm 2.1$  is used (Freedman et al. 2012). The cut-off scenarios are indicated in the figure labels (a) to (c).

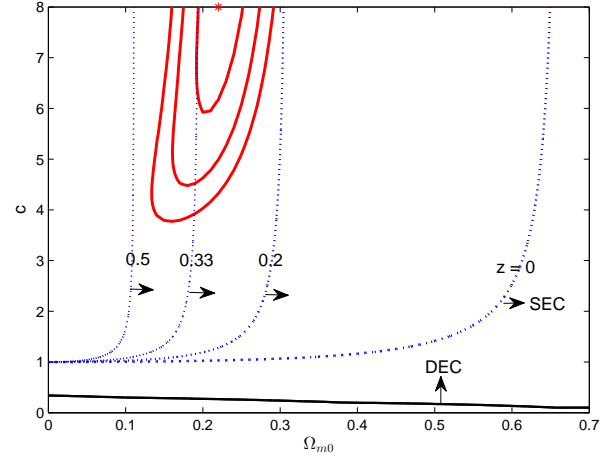


**Figure 2.** Observational constraints and the energy condition bounds for the cosmic age cut-off. The solid contours correspond to the joint constraint from OHD and SN data. Energy conditions bounds are labeled by redshift, and arrows point to the direction where the conditions are (or use to be) fulfilled. NEC bounds cover the whole parameter space, which is too trivial to be plotted. Constraint from SEC changes evidently with redshift, but constraint from DEC barely changes. Since constraints from the energy conditions are redshift dependent, i. e. constraints on  $\Omega_m(z)$ , we have transferred the unit into the current parameter space  $(\Omega_{m0}, c)$  according to the evolution of matter.

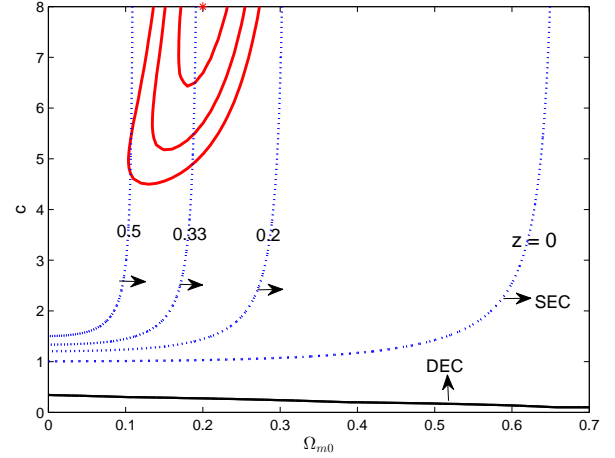


**Figure 3.** Same as Figure 2 but for the conformal time cut-off. Analogous results for SEC are obtained.

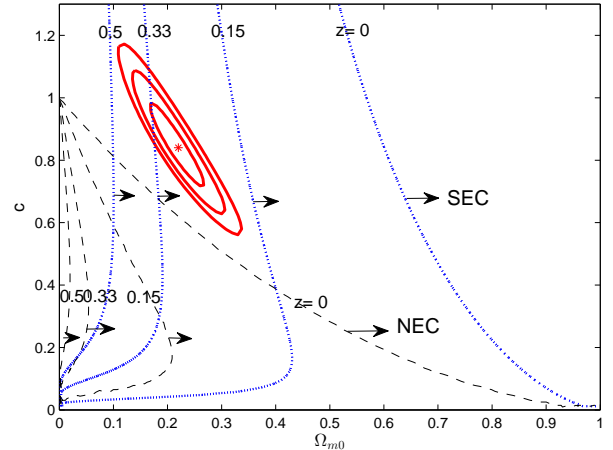


**Figure 4.** Same as Figure 2 but for the event horizon cut-off. Dashed curves show the boundaries of constraint from NEC.

conformal time cut-off. As discussed above, these two models eventually approaches the  $\Lambda$ CDM model. The constant  $c = 0.84^{+0.14}_{-0.12}$  is obtained from joint data constraint for the event horizon cut-off, which shows its difference from the  $\Lambda$ CDM model.

The energy conditions turn out an useful approach to the study of cosmology, because of its model independence and universality. In our analysis, we superimpose the energy conditions bounds on the constraints from observational data as done in Figures 2, 3, and 4 at different redshift. In these scenarios, we find that SEC is fulfilled at redshift  $z \gtrsim 0.3$  with  $1\sigma$  confidence level, and  $z \gtrsim 0.5$  with  $3\sigma$  confidence level, which is well consistent with the result reported by Wu et al. (2012). Note that SEC is violated currently, which is expected (Lima et al. 2008; Wu et al. 2012). Moreover, we find that NEC can provide an additional constraint on  $\Omega_{m0}$  and constant  $c$  for the event horizon cut-off, when it is compared with OHD only. For example, joint constraint from OHD and NEC shows that constant  $c$  should fall within (0.45, 1.3) at  $1\sigma$  confidence level. This also presents the constraint ability of NEC when compared with some data.

Compared with the work of Wu et al. (2012), our results are obtained from a much narrower class of models. It should be noted that their work assumed a family of discontinuous functions as the bases on which the kinematic terms are expanded. Our result, in contrast, is not subjected to this limitation. Therefore our analysis cannot be viewed as a special case of theirs. Nevertheless, we are able to confirm the major features of their results, namely the fulfilment of DEC and the violation of SEC. Our method can be used to better pinpoint the onset of SEC violation, and is less ambiguous at higher redshift.

It is possible, according to our results, to distinguish NEC as the energy condition *primus inter pares*. The interesting feature of NEC can be summarized as follows. For models that cannot be well-constrained by the data, we find that NEC will also fail to constrain, yielding too generous a bound. For the model capable of being constrained by data, NEC gives a meaningful constraint that is neither in conflict with, nor entirely implied by the data. This feature is neither shared by SEC, which tends to be violated, nor DEC, which always give trivial bounds. In future analysis of other dark energy proposals, therefore, NEC may be a worthwhile theoretical consideration before the application of data analysis.

However, we must note that the data used in this paper are certainly to be updated in the future, and the relation between data- and NEC-bounds remains an open topic. Future data with less statistical uncertainty could, in principle, reduce the need of applying an NEC bound. Meanwhile, it may better confirm the validity of NEC for all cosmic ages, strengthening its role as the “special” energy condition for cosmology.

This work was supported by the National Science Foundation of China (grant No. 11173006), the Ministry of Science and Technology National Basic Science program (project 973) under grant No. 2012CB821804, and the Fundamental Research Funds for the Central Universities.

## REFERENCES

- Amanullah, R., Lidman, C., Rubin, D., et al. 2010, *ApJ*, 716, 712  
 Armendariz-Picon, C., Mukhanov, V., & Steinhardt, P. 2000, *Phys. Rev. Lett.*, 85, 4438  
 Bhattacharya, s., & Debnath, U. 2011, *International Journal of Modern Physics D*, 20, 1191  
 Caldwell, R., Kamionkowski, M., & Weinberg, N. 2003, *Phys. Rev. Lett.*, 91, 71301  
 Carroll, S. 2004, *Spacetime and geometry* (Addison-Wesley, Pearson)  
 Cattoën, C., & Visser, M. 2008, *Class. Quantum Grav.*, 25, 165013  
 Chen, Y., Zhu, Z.H., Xu, L., & Alcaniz, J. 2011, *Phys. Lett. B*, 698, 175  
 Cohen, A., Kaplan, D., & Nelson, A.E. 1999, *Phys. Rev. Lett.*, 82, 4971  
 Di Pietro, E., & Claeskens, J.F. 2003, *MNRAS*, 341, 1299  
 Enqvist, K., Hannestad, S., & Sloth, M. 2005, *JCAP*, 02, 004  
 Epstein, H., Glaser, V. & Jaffe, A. 2007, *Nuovo Cimento*, 36, 1016–1022  
 Feng, B., Wang, X., & Zhang, X. 2005, *Phys. Lett. B*, 607, 35  
 Fewster, C.J., & Eveson, S.P. 1998, *Phys. Rev. D*, 58, 084010  
 Freedman, W.L., Madore, B.F., Scowcroft, V., et al. 2012, *ApJ*, 758, 24  
 Gaztanaga, E., Cabré, A., & Hui, L. 2009, *MNRAS*, 399, 1663  
 Hawking, S., & Ellis, G. 1975, *The large scale structure of space-time* (Cambridge University Press)  
 Huang, Q., & Gong, Y. 2004, *JCAP*, 0408, 006  
 Jimenez, & Loeb, A. 2002, *ApJ*, 573, 37  
 Kao, H.C. and Lee, W.L. & Lin, F.L. 2002, *Phys. Rev. D*, 71, 123518  
 Kim, K.Y. Lee, H.W. & Myung, Y.S. 2008, *Phys. Lett. B*, 660, 118  
 Lima, M., Vinenti, S., & Rebouças, M. 2008, *Phys. Rev. D*, 77, 083518  
 Li, M. 2004, *Phys. Lett. B*, 603, 1  
 Li, M., Li, X., Wang, S., & Wang, Y. 2011, *Communications in Theoretical Physics*, 56, 525  
 Lin, H., Hao, C., Wang, X., et al. 2009, *Mod. Phys. Lett. A*, 24, 1699  
 Ma, C., & Zhang, T.J. 2011, *ApJ*, 730, 74  
 Moresco, M., Cimatti, A., Jimenez, R. et al. 2012, *JCAP*, 08, 006  
 Myung, Y., & Seo, M. 2009, *Phys. Lett. B*, 671, 435  
 Nesseris, S., Perivolaropoulos, L., 2005, *Phys. Rev. D*, 72, 123519  
 Nishizawa, A., Taruya, A., & Saito, S. 2011, *Phys. Rev. D*, 83, 084048  
 Padmanabhan, T., 2002, *Phys. Rev. D*, 66, 021301  
 Peebles, P., & Ratra, B. 1988, *ApJ*, 325, L17  
 Perivolaropoulos, L. 2005, *Phys. Rev. D*, 71, 063503  
 Piazza, F., & Tsujikawa, S. 2004, *JCAP*, 2004, 004  
 Riess, A., et al., 1998, *ApJ*, 116, 1009  
 Samushia, L., & Ratra, B. 2006, *ApJ*, 650, L5  
 Schuecker, P., Caldwell, R., et al. 2003, *A&A*, 402, 53  
 Setare, M., 2006, *Phys. Lett. B*, 642, 1  
 Simon, J., Verde, L., & Jimenez, R. 2005, *Phys. Rev. D*, 71, 123001  
 Spergel, D., et al., 2003, *ApJS*, 148, 170  
 Stern, J., Jimenez, R., & Verde, L., et al. 2010, *JCAP*, 02, 008  
 Susskind, L. 1995, *Journal of Mathematical Physics*, 36, 6377  
 Tegmark, M., et al. 2004, *Phys. Rev. D*, 69, 103501  
 't Hooft, G. 2001, *Basics and Highlights in Fundamental Physics*, 1, 72  
 Visser, M. 1997, *Science*, 276, 88  
 Visser, M. 1997, *Phys. Rev. D*, 56, 7578  
 Visser, M. & Barcelo, C. 2000, *arXiv:gr-qc/0001099v1*  
 Wald, R. 1984, *General relativity* (University of Chicago press)  
 Wang, H., & Zhang, T.J. 2012, *ApJ*, 748, 111  
 Wu, C.J., Ma, C., & Zhang, T.J. 2012, *ApJ*, 753, 97  
 Wu, Q., Gong, Y., Wang, A., & Alcaniz, J. 2008, *Phys. Lett. B*, 659, 34  
 Xu, L., Lu, J., & Li, W. 2010, *Phys. Lett. B*, 690, 333  
 Yi, Z.L., & Zhang, T.J. 2007, *Mod. Phys. Lett. A*, 22, 41  
 Zhai, Z.X., Zhang, T.J., & Liu, W.B. 2011, *JCAP*, 08, 019  
 Zhang, C., Zhang, H., Yuan, S., et al. 2012, *arXiv:1207.4541v1*  
 Zhang, T.J., Ma, C., & Lan, T. 2010, *Advances in Astronomy*, 2010, 81  
 Zhang, X., & Wu, F. 2007, *Phys. Rev. D*, 76, 023502